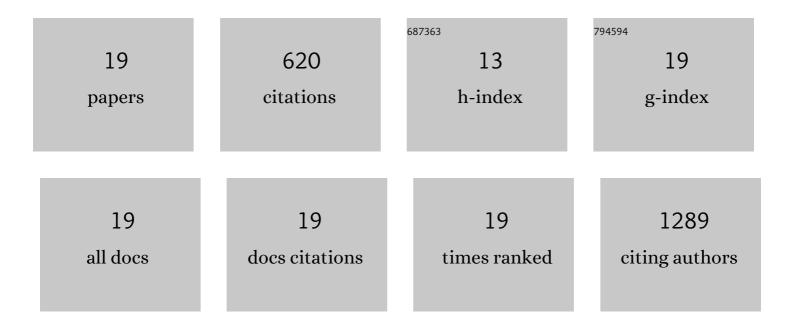
## R Mark Simpson

List of Publications by Year in descending order

Source: https://exaly.com/author-pdf/1845794/publications.pdf Version: 2024-02-01



#	Article	IF	CITATIONS
1	Sporadic naturally occurring melanoma in dogs as a preclinical model for human melanoma. Pigment Cell and Melanoma Research, 2014, 27, 37-47.	3.3	112
2	A Revised Diagnostic Classification of Canine Glioma: Towards Validation of the Canine Glioma Patient as a Naturally Occurring Preclinical Model for Human Glioma. Journal of Neuropathology and Experimental Neurology, 2018, 77, 1039-1054.	1.7	105
3	Naturally Occurring Canine Melanoma as a Predictive Comparative Oncology Model for Human Mucosal and Other Triple Wild-Type Melanomas. International Journal of Molecular Sciences, 2018, 19, 394.	4.1	78
4	Synergistic targeted inhibition of <scp>MEK</scp> and dual <scp>PI</scp> 3K/ <scp>mTOR</scp> diminishes viability and inhibits tumor growth of canine melanoma underscoring its utility as a preclinical model for human mucosal melanoma. Pigment Cell and Melanoma Research, 2016, 29, 643-655.	3.3	43
5	Integrative Genomic and Transcriptomic Characterization of Matched Primary and Metastatic Liver and Colorectal Carcinoma. International Journal of Biological Sciences, 2015, 11, 88-98.	6.4	37
6	The Protein Phosphatase 2A Inhibitor LB100 Sensitizes Ovarian Carcinoma Cells to Cisplatin-Mediated Cytotoxicity. Molecular Cancer Therapeutics, 2015, 14, 90-100.	4.1	36
7	High-throughput screens identify HSP90 inhibitors as potent therapeutics that target inter-related growth and survival pathways in advanced prostate cancer. Scientific Reports, 2018, 8, 17239.	3.3	29
8	TORC1 and class I HDAC inhibitors synergize to suppress mature B cell neoplasms. Molecular Oncology, 2014, 8, 261-272.	4.6	25
9	Digital pathology and image analysis augment biospecimen annotation and biobank quality assurance harmonization. Clinical Biochemistry, 2014, 47, 274-279.	1.9	23
10	Nuclear pore protein NUP210 depletion suppresses metastasis through heterochromatin-mediated disruption of tumor cell mechanical response. Nature Communications, 2021, 12, 7216.	12.8	19
11	cFOS-SOX9 Axis Reprograms Bone Marrow-Derived Mesenchymal Stem Cells into Chondroblastic Osteosarcoma. Stem Cell Reports, 2017, 8, 1630-1644.	4.8	17
12	Agreement in Histological Assessment of Mitotic Activity Between Microscopy and Digital Whole Slide Images Informs Conversion for Clinical Diagnosis. Academic Pathology, 2019, 6, 2374289519859841.	1.1	16
13	The Outcome of TGFβ Antagonism in Metastatic Breast Cancer Models <i>In Vivo</i> Reflects a Complex Balance between Tumor-Suppressive and Proprogression Activities of TGFβ. Clinical Cancer Research, 2020, 26, 643-656.	7.0	16
14	Functional Analysis of Prognostic Gene Expression Network Genes in Metastatic Breast Cancer Models. PLoS ONE, 2014, 9, e111813.	2.5	15
15	Efficacy, Tolerability, and Pharmacokinetics of Combined Targeted MEK and Dual mTORC1/2 Inhibition in a Preclinical Model of Mucosal Melanoma. Molecular Cancer Therapeutics, 2020, 19, 2308-2318.	4.1	14
16	Automated Computational Detection, Quantitation, and Mapping of Mitosis in Whole-Slide Images for Clinically Actionable Surgical Pathology Decision Support. Journal of Pathology Informatics, 2019, 10, 4.	1.7	13
17	Bioluminescent imaging of ABCG2 efflux activity at the blood-placenta barrier. Scientific Reports, 2016, 6, 20418.	3.3	8
18	In Vivo Bioluminescent Imaging of ATP-Binding Cassette Transporter-Mediated Efflux at the Blood–Brain Barrier. Methods in Molecular Biology, 2016, 1461, 227-239.	0.9	7

#	Article	IF	CITATIONS
19	Hypomorphic mTOR Downregulates CDK6 and Delays Thymic Pre-T LBL Tumorigenesis. Molecular Cancer Therapeutics, 2020, 19, 2221-2232.	4.1	7